

3D Porous Ni-Cu Alloy Film for High-performance Hydrazine

Electrooxidation

Ming Sun, Zhiyi Lu, Liang Luo*, Zheng Chang*, Xiaoming Sun

Supporting information

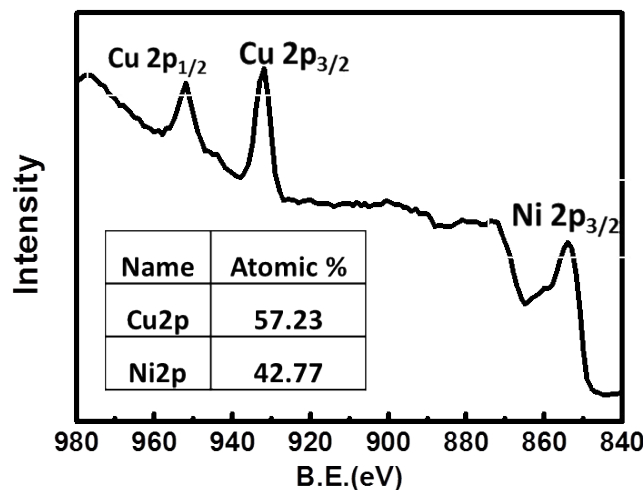


Fig. S1 Cu 2p_{1/2}, Cu 2p_{3/2} and Ni 2p_{3/2} orbital binding energy regions in the full XPS spectrum of the optimal Ni–Cu alloy film and the calculated Cu/Ni atomic ratio of 1.34/1.

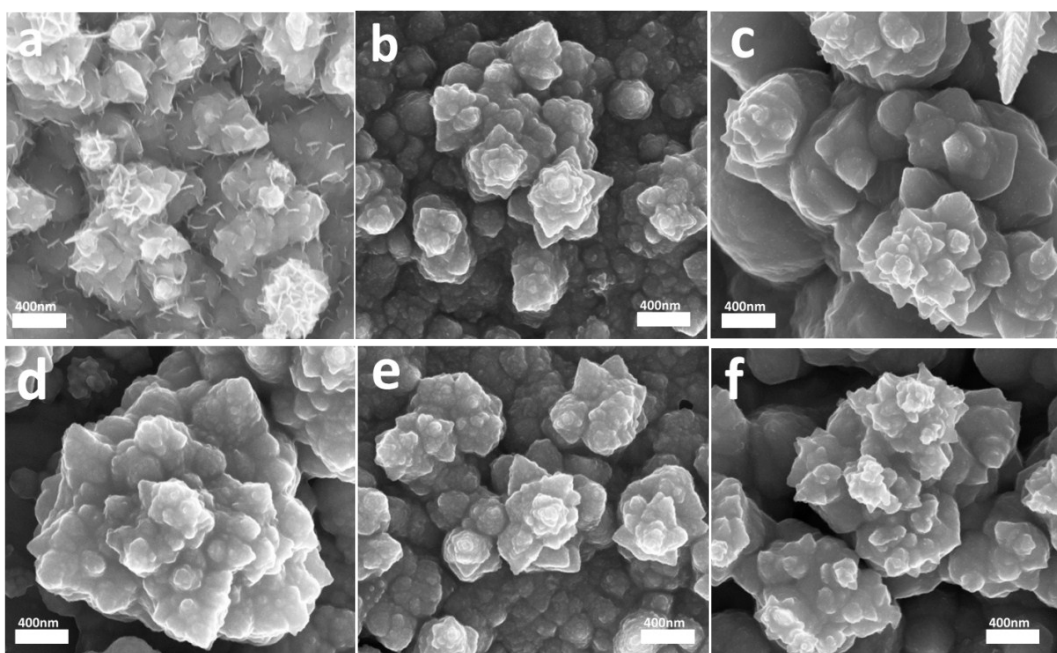


Fig. S2 SEM images of the Ni-Cu alloy films prepared at the different electrode position potentials for the same time of 400 s: a) -1.2 V; b) -1.5 V; c) -1.9 V and prepared at the same potential of -1.8 V for the different electrode position time: d) 100 s; e) 200 s; f) 600 s.

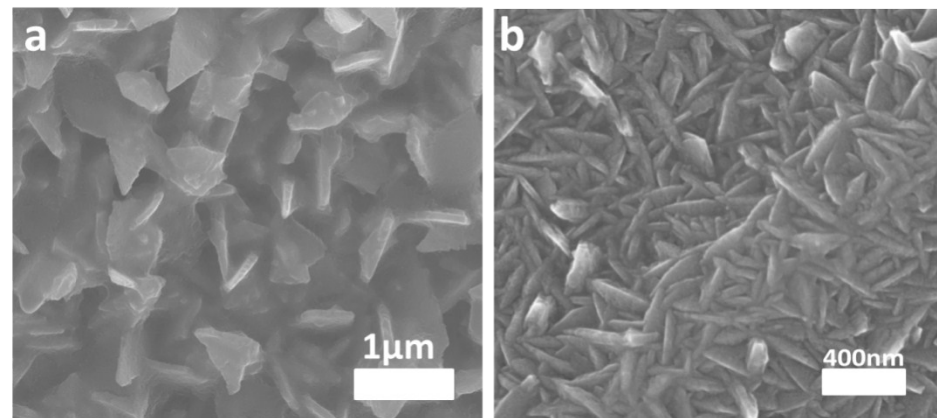


Fig. S3 SEM images of control samples: a) Cu array film; b) Ni array film.

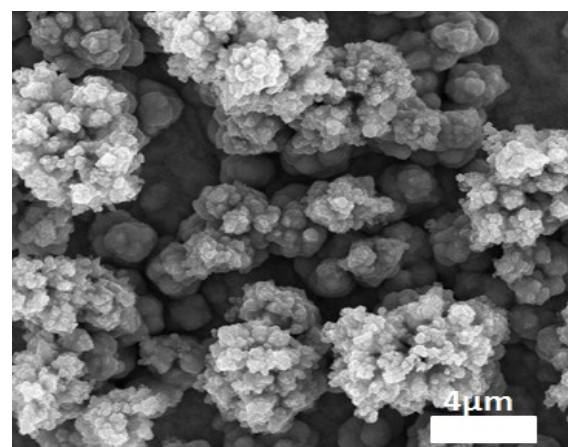


Fig. S4 SEM image of the optimal Ni-Cu alloy film after a long time stability testing.

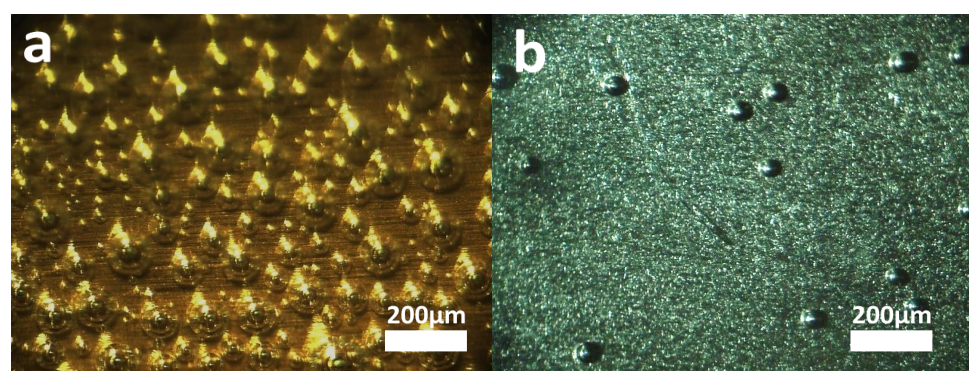


Fig. S5 The digital images showing the bubble generation behaviors on a) Cu foil and b) Ni foil.

Table S1 HzOR performance comparison of the Ni-based alloys in our work and some references.

Sample	Conditions	Current density	Stability	Ref.
Highly metallic Ni NPs	0.1M N ₂ H ₄ , 0.1M NaOH	608 A g ⁻¹ at 0.1V (vs. RHE)	—	31
Ni ₈₅ Fe ₁₅ /PEI-MoS ₂	0.1M N ₂ H ₄ , 0.15M NaOH, 60°C	520 A g ⁻¹ at -0.2V (vs. SCE)	~30%	29
Ni _{0.33} Zn _{0.67}	5% N ₂ H ₄ , 1M KOH, 60°C	500 A g ⁻¹ at 0.35V (vs. RHE)	—	22
Ni ₅₅ Fe ₄₅	0.1M N ₂ H ₄ , 0.015M KOH, 60°C	350 A g ⁻¹ at -0.4V (vs. RHE)	—	33
Ni-Mn(Fe, Zn)/C	1M N ₂ H ₄ , 1M KOH, 60°C	200 A g ⁻¹ at 0.2V (vs. RHE)	—	34
Ni _{0.4} La _{0.6} /C	1M N ₂ H ₄ , 1M KOH, 60°C	88.6 A g ⁻¹ at 0.22V (vs. RHE)	—	30
Ni-Zr	2M N ₂ H ₄ , 1M NaOH	165 mA cm ⁻² at -0.8V (vs. NHE)	—	28
Ni ₈₀ Fe ₂₀ /PEI-rGO _{10:1}	0.1M N ₂ H ₄ , 0.15M NaOH	57 mA cm ⁻² at 0.5V (vs. SCE)	~17%	32
Ni ₁ Co ₁	0.1M N ₂ H ₄ , 1M KOH, 60°C	36 mA cm ⁻² at 0.1V (vs. RHE)	39%	35
Ni _{0.87} Zn _{0.13} /C	0.1M N ₂ H ₄ , 1M KOH	5 mA cm ⁻² at 0.35V (vs. RHE)	—	23
Ni _{0.43} Cu _{0.57}	0.1M N ₂ H ₄ , 3M NaOH	300 mA cm ⁻² at -0.6V (vs. SCE)	80%	This work